EUROPEAN ORGANIZATION FOR NUCLEAR RESEARCH

CERN-EP/85-189
November 21st, 1985

A STUDY OF THREE-JET EVENTS AT THE CERN $\bar{p}p$ COLLIDER

The UA2 Collaboration

Bern[1] - CERN[2] - Copenhagen (NBI)[3] - Heidelberg[4] - Orsay (LAL)[5] - Pavia[6] - Perugia[7] - Pisa[8] - Saclay (CEN)[9] Collaboration

J.A. Appel[9,a], P. Bagnaia[2], M. Banner[9], R. Battiston[7], K. Bernlöhr[4], K. Borer[1], M. Borghini[2], J. Bürger[2,b], G. Carboni[8], V. Cavasinni[8], P. Cenci[7,c], J.-C. Chollet[5], A.G. Clark[2], A. Codino[7], C. Conta[6], P. Darriulat[2], B. De Lotto[5], T. Del Prete[8], L. Di Lella[2], J. Dines-Hansen[3], K. Einsweiler[2], R. Engelmann[2,d], L. Fayard[5], M. Fraternali[6], D. Froidevaux[5], J.-M. Gaillard[5], O. Gildemeister[2], V.G. Goggi[6], C. Gössling[2], B. Hahn[1], H. Hänni[2], J.R. Hansen[2], P. Hansen[2,3], N. Harnew[2], T. Himel[2,e], L. Iconomidou-Fayard[5], K. Jakobs[4], P. Jenni[2], E.E. Kluge[4], O. Kofoed-Hansen[3], E. Lançon[9], M. Livan[6], S. Loucatos[9], B. Madsen[3], P. Mani[1], B. Mansoulié[9], G.C. Mantovani[7], L. Mapelli[2,f], K. Meier[2], B. Merkel[5], R. Mollerud[3], M. Moniez[5], R. Moning[1], M. Morganti[8], C. Onions[2], M.A. Parker[2], G. Parrour[5], F. Pastore[6], M. Pepe[7], H. Plothow-Besch[4], M. Polverel[9], J.-P. Repellin[5], A. Rimoldi[6], A.F. Rothenberg[2,e], A. Roussarie[9], V. Ruhlmann[9], G. Sauvage[5], J. Schacher[1], M. Schlötelburg[4], F. Stocker[1], M. Swartz[2], J. Teiger[9], S.N. Tovey[2,g], W.Y. Tsang[h], M. Valdata-Nappi[8], V. Vercesi[6], A.R. Weidberg[2], M. Wunsch[4] and H. Zaccone[9].

(Submitted to Zeitschrift für Physik C - Particles and Fields)

ABSTRACT

The UA2 experiment, running at the CERN SPS $\bar{p}p$ Collider, has performed a study of events containing three hard jets in the final state. The angular distributions of the three jets show evidence for gluon bremsstrahlung, in good agreement with a QCD model to leading order in the strong coupling constant α_s. The yield of three-jet events relative to that of two-jet events provides a measure of the strong coupling constant : $\alpha_s K_3/K_2 = 0.23 \pm 0.01 \pm 0.04$, where K_2 and K_3 represent the contributions arising from higher order corrections in α_s to the two- and three-jet exclusive cross-sections. A detailed discussion of the systematic and theoretical uncertainties is given.

---

1. Laboratorium für Hochenergiephysik, Universität Bern, Sidlerstrasse 5, Bern, Switzerland.
2. CERN, 1211 Geneva 23, Switzerland.
3. Niels Bohr Institute, Blegdamsvej 17, Copenhagen, Denmark.
4. Institut für Hochergiephysik der Universität Heidelberg, Schröderstrasse 90, 6900 Heidelberg, FRG.
5. Laboratoire de l'Accélérateur Linéaire, Université de Paris-Sud, Orsay, France.
6. Dipartimento di Fisica Nucleare e Teorica, Università di Pavia and INFN, Sezione di Pavia, Via Bassi 6, Pavia, Italy.
7. Gruppo INFN del Dipartimento di Fisica dell'Università di Perugia, Italy.
8. Dipartimento di fisica dell'Università di Pisa and INFN, Sezione di Pisa, Via Livornese, S. Piero a Grado, Pisa, Italy.
9. Centre d'Etudes Nucléaires de Saclay, France.
a) On leave from FNAL, Batavia, USA.
b) On leave from DESY, Hamburg, FRG.
c) Also at Scuola Normale Superiore, Pisa, Italy.
d) On leave from New York State University, Stony Brook, NY, USA.
e) Now at SLAC, Stanford University, Stanford, USA.
f) On leave from INFN, Pavia, Italy.
g) Visitor from the University of Melbourne, Australia.
h) Cavendish Laboratory, University of Cambridge, Cambridge, UK.

which a cluster pair is first resolved is a sharply defined, energy-independent quantity. In a first phase of analysis, primary clusters are obtained by simply connecting all adjacent cells having an energy in excess of a 400 MeV threshold. In a second phase, the clusters are reprocessed using the same algorithm, but applying a higher threshold, set at 5% of the total energy of the primary cluster. The content of a primary cluster cell whose energy is below the new threshold is redistributed among secondary clusters according to their relative location and energy content. We have studied the angular resolving power associated with this refined algorithm by superimposing jets obtained from two different two-jet events. The fraction of such events for which the clustering algorithm finds two clusters is a measure of the angular resolving power. It is found to have a distribution with an approximately energy-independent cut-off at $30° \pm 10°$ (Figure 1).

A momentum vector is associated with each cluster using the approximation that its mass is zero. Its direction is given by the line joining the centre of the UA2 detector to the cluster centroid and its length is measured by the cluster energy. In this approximation, the cluster transverse momentum vector (the projection of the momentum vector on a plane normal to the beam line), has a length measured by the cluster transverse energy, E_T.

In each event, the clusters are sorted in order of decreasing transverse energy and labeled 1, 2, 3, etc. For events in which the two leading clusters alone satisfy the trigger condition, $(E_T^1 + E_T^2 \geq 60$ GeV), the average transverse energy of the third cluster is $\cong 5$ GeV, nearly independent of $E_T^1 + E_T^2$. This represents $\simeq 27\%$ of the total transverse energy complementary to that of the leading jet pair, $\langle \tilde{E}_T \rangle = \langle \Sigma E_T - E_T^1 - E_T^2 \rangle \simeq 17.5$ GeV [16]. However, in a significant fraction of the events, the third cluster has a transverse energy much larger than this average value. This is illustrated in Figure 2 where the probability P_ϵ that an event contains a third cluster having E_T^3 in excess of ϵ is shown as a function of $E_T^1 + E_T^2$ for various values of ϵ. This Figure demonstrates the existence of a significant event sample with at least three hard jets in the final state.

In the remainder of the present article we shall study such events, subject to the conditions

$$E_T^1 + E_T^2 + E_T^3 > 70 \text{ GeV}, \tag{1a}$$

$$E_T^3 > 10 \text{ GeV}, \quad E_T^4 < 10 \text{ GeV}, \tag{1b}$$

$$|\eta_i| < 0.80, \quad i = 1,2,3. \tag{1c}$$

The first condition ensures that the configuration of the three leading jets is unbiased by the trigger threshold. The second condition retains events in which the third cluster is likely to be associated with the hard collision rather than with spectator fragments (the condition on E_T^4 is an exclusive topology selection). The third condition defines a fiducial volume in which the jet energy measurements are reliable. There are 6223 events which satisfy the above conditions. Similarly we define a sample of two-jet events in which conditions (1) are replaced by

$$E_T^1 + E_T^2 > 70 \text{ GeV}, \tag{2a}$$

$$E_T^2 > 10 \text{ GeV}, \quad E_T^3 < 10 \text{ GeV}, \tag{2b}$$

$$|\eta_i| < 0.80, \quad i = 1,2. \tag{2c}$$

respectively. This sample contains 13346 events.

For each event in the two-jet (or three-jet) samples just defined, we calculate the transverse momentum P_T of the jet system as the vector sum of the transverse momenta of the leading two (or three) clusters. The distributions of P_T for the two-jet and three-jet samples are displayed in Figure 3.

1. INTRODUCTION

The CERN $\bar{p}p$ Collider is an excellent laboratory for the study of short distance (hard) collisions between nucleon constituents (quarks and gluons). Such collisions have been the subject of extensive studies and their properties have been successfully compared with the predictions of perturbative quantum chromodynamics (QCD) [1-12]. This is made possible by the presence of hadron jets which can be isolated from the other collision products and identified with the outgoing partons. In particular, most features of two-jet final states are well described by the leading term in the perturbative expansion of the parton-parton cross-section in powers of the strong coupling constant α_s. The next term implies the existence of three-jet final states in which a gluon has been radiated. The observation [2,12] and detailed study of the properties of these final states is a crucial test of the theory and is the subject of the present article. We divide this study into two areas of investigation. First, the configuration of the events is studied. The shapes of the relevant distributions are compared both with a QCD model and with phase space, in order to test the underlying dynamics. These comparisons confirm the qualitative features expected of QCD, in particular, a Rutherford-like angular dependence for the scattering angle of the leading jet and a bremsstrahlung spectrum for the energy and angle of the softest jet. This agreement encourages us to perform more quantitative tests of QCD. To do so, we measure the cross-section for the production of three-jet events relative to that for two-jet events.

The two-jet and three-jet production cross-sections are approximately proportional to α_s^2 and α_s^3 respectively. In principle, an evaluation of α_s can be made from the measurement of one or the other of these two quantities. In practice, it cannot be done with sufficient accuracy because important uncertainties are attached to jet cross-section measurements (due particularly to experimental uncertainties on the energy scale), to the evaluation of higher order terms (K-factors), and to the gluon structure function extrapolated from low-q^2 leptoproduction experiments. However, these uncertainties largely cancel in the ratio between the two cross-sections, whose measurement therefore provides a means of evaluating α_s. The comparison between the result of such an evaluation and the value obtained from e^+e^- experiments [13] is very instructive to the extent that the two methods are associated with different sources of systematic uncertainties : fragmentation effects have become less important at Collider energies, but we have to cope with the complexity arising from the presence of many competing parton subprocesses and with collision products from spectator fragmentation.

2. THE DATA

The data for the present study have been obtained using the UA2 central calorimeter [14] which covers the pseudo-rapidity region $-1 \leq \eta \leq +1$ over the whole azimuthal range. Its high granularity (240 cells, each covering 15° in azimuth and 10° in polar angle) is well matched to the jet structure of hard collision final states at Collider energies. The trigger is obtained from a coincidence between a minimum bias signal [15], ensuring the occurrence of a non-diffractive $\bar{p}p$ collision, and the requirement that ΣE_T, the total transverse energy measured in the 240 calorimeter cells, exceeds 60 GeV. The data were collected at $\sqrt{s} = 630$ GeV and correspond to a total integrated luminosity of 310 nb^{-1}.

A small background contamination, resulting from the interactions of beam halo particles in the UA2 calorimeter, is reduced to a negligible level (< 2% independently of ΣE_T) after the application of sharp timing cuts and rejection of events having characteristic background configurations in their pattern of energy deposition [2-6].

In each event, energy clusters are constructed using a refined algorithm optimized for the study of three-jet final states. In these events, the opening angle of one of the jet pairs is often small, as a result of gluon bremsstrahlung. For this reason, special care is devoted to ensuring that the opening angle at

A number of experimental effects contribute to these distributions : the resolution of the calorimeter energy measurement, the presence of hard collision products outside the detector acceptance, etc. They were discussed for the two-jet case in a previous publication [4]. However, even in the case of a perfect detector, P_T is expected to deviate significantly from zero as the result of higher order soft gluon corrections to the leading order QCD diagrams [17]. The strong similarity between the P_T distributions of the two-jet and three-jet samples (Figure 3) leads us to assume that these effects can be ignored as long as we exclude those events which fall in the tails of the P_T distributions. In what follows, we submit the two-jet and three-jet samples to the additional condition

$$P_T < 20 \text{ GeV} \qquad (3)$$

and perform a transverse Lorentz transformation on each event to bring the jet system to rest in the transverse plane. In the subsequent analysis we shall verify that our conclusions are insensitive to the effects of this Lorentz boost. As a result of this transformation, we now deal with two-jet and three-jet samples having $P_T = 0$. They contain 10566 events and 4972 events respectively. By an obvious extension of our selection criteria (1 and 3), we define a four-jet sample, which contains 961 events.

3. THE QCD MODEL

The present study relies on comparisons between experimental distributions associated with the three-jet sample and the corresponding QCD predictions. It is therefore necessary to describe, in detail, the QCD model and its implementation in a Monte Carlo simulation of the UA2 detector.

To leading order in α_s, the cross-section for producing n final state partons with a total invariant mass $\sqrt{\hat{s}}$ is expressed in terms of elementary subprocesses in which two incident partons, i and j, carrying fractions x_i and x_j of their nucleon parent momentum, interact :

$$\sigma_n^{LO} = ([\alpha_s]^n/\hat{s}) \int \Sigma_{ij} F_i(x_i) F_j(x_j) Q_n^{ij} \Phi_n (dx_i/x_i) (dx_j/x_j) \qquad (4)$$

where Φ_n is the n-body phase-space factor and $x_i x_j s = \hat{s}$.

Explicit expressions for the contribution Q_n^{ij} of each elementary subprocess are available in the literature for n = 2 [18] and n = 3 [19]. In Equation (4), they are weighted according to the structure functions $F_i(x)$ which describe the parton content of the incident nucleons.

As a result of the bremsstrahlung nature of the gluon radiation spectrum, Q_n^{ij} diverges when the mass of any two partons, one from the final state and one from either the initial or final state, approaches zero. These divergences are cancelled by non-leading contributions to the topological cross-sections associated with lower parton multiplicities in the final state. This feature, inherent in QCD, is closely related to the existence of hadron jets having angular apertures of order α_s [20]. It restricts the validity of perturbative QCD descriptions to final states in which the initial and final state partons are well separated in phase-space.

We implement this requirement in our model by defining cut-offs to ensure that the parton configuration in the final state is free of these divergences : we only consider partons having a transverse momentum in excess of 8 GeV and parton pairs having a separation in excess of 40°. With these cut-offs, the ratio K_n between the topological cross-section σ_n and its leading order approximation σ_n^{LO} can, in principle, be computed, although the necessary calculations have not yet been performed. The values of K_2 and K_3 should depend on the choice of the cut-offs. However, experience with other processes [21] and simple arguments using dimensional regularization [22] suggest that K_n may be approximately independent of the final state configuration and take values

between 1 and 2. Lacking a precise calculation of K_n we shall have to compare the two-jet and three-jet data to expressions proportional to $K_2\,\alpha_s^2$ and $K_3\,\alpha_s^3$ respectively, with the result that the ratio of cross-sections is sensitive to the quantity $\alpha_s K_3/K_2$, instead of simply α_s.

Two additional comments are required to clarify Equation (4) :

i. the quark and antiquark structure functions, $Q(x)$ and $\bar{Q}(x)$, are taken from low q^2 neutrino data [23] evolved to the q^2-range of the present experiment [24]. The gluon structure function is taken to be

$$G(x) = F(x)/\sqrt{K} - 4/9\,[Q(x) + \bar{Q}(x)] \qquad (5)$$

where $F(x)$ is the effective structure function obtained from the two-jet data of the UA2 experiment [4]. In this evaluation, we assume that the inclusive K-factor takes the value $K = 2$ and we shall account for the effects of this assumption when evaluating the systematic uncertainties of the final result.

ii. scaling violations are expressed by terms of the form $\ell n\,(q^2/\Lambda^2)$, where Λ is the QCD scale parameter. We choose to identify $\sqrt{q^2}$ with the largest transverse momentum among the final state partons. The strong coupling constant α_s is a function of q^2,

$$\alpha_s = 12\pi/[(33-2N_f)\,\ell n\,(q^2/\Lambda^2)] \qquad (6)$$

where Λ is the QCD scale parameter and N_f, the number of relevant flavours, is taken to be 5. Though our definition of q^2 is somewhat arbitrary, the direct result of our measurement is an effective coupling constant in the q^2-range relevant to the present experiment. A different definition of q^2 might yield another value for Λ but would not change α_s significantly, provided that it affects the q^2-range for the two-jet and three-jet cross-sections in a similar way. The use of a different definition of q^2, which does not have this property, and the expected variation of α_s with q^2 in our data sample are discussed in Section 5.

In order to convert the final state partons of Equation (4) into observable hadrons, we use a fragmentation method based on the Field-Feynman algorithm [25], modified to reproduce the cluster radius distribution observed in the present experiment [2]. We have checked that this method of fragmentation, when used in conjunction with the clustering algorithm described in Section 2 and 5, produces extra clusters in less than 2% of the events for cluster transverse energies in excess of 15 GeV. This empirically demonstrates that in the model the radiation of hard partons can be separated from the soft fragmentation process, and ensures that the jets in the final state arise from the hard-scattering matrix element and not from the fragmentation model. In addition, the effects of heavy flavour fragmentation are neglected in our model since they are not expected to give a significant contribution to the three-jet sample.

The acceptance of the UA2 detector and the details of the energy response of the central calorimeter are simulated in a Monte Carlo programme which reproduces the experimental details of relevance [2]. The underlying event, associated with spectator particles, is simulated by superimposing onto the jets produced by the hard collision actual minimum bias events, scaled in energy so as to reproduce the measured value of $\tilde{E}_T$.

We evaluate the topological cross-sections σ_n^{LO} in the QCD model from the Monte Carlo sample, submitted to the same selection criteria (1-3) as the data. In the following we shall compare the measured cross-sections, σ_2 and σ_3, with σ_2^{LO} and σ_3^{LO}. We note that σ_2 and σ_3 are not inclusive cross-sections, namely events containing ≥ 3 (4) observed hard jets in the final state are excluded from

the sample of two(three)-jet events used to evaluate σ_2 (σ_3). However, the limited acceptance and resolving power of the UA2 detector causes some n-jet final states to be observed as m-jet events, $m < n$. We use the available expressions for Q_2^{ij} and Q_3^{ij} to evaluate this effect in the corresponding topologies. The lack of a similar expression for Q_4^{ij} precludes an accurate evaluation of the contamination of four-jet events in the samples containing 2 or 3 jets observed in the detector. To overcome this difficulty, we use an ad-hoc model in which three-jet final states described by Equation (4) are transformed into four-jet final states by radiating a gluon from one of the initial or final state partons. The bremsstrahlung probability is taken to be of the form [26] corresponding to three-jet final states in e^+e^- collisions and normalized to provide an adequate description of four-jet final states in which all four jets are observed in the UA2 detector.

4. DESCRIPTION OF THE THREE−JET SAMPLE AND COMPARISON WITH THE QCD MODEL

In this Section we study the event configurations for a three-jet sample selected according to the criteria (1) and (3). Having set $P_T = 0$ by application of the appropriate Lorentz boost, we are left with three jets of invariant mass M having a total momentum P_L parallel to the beams. In the ideal case where the three jet momenta are identical to the three parton momenta, M and P_L are simply related to the momenta $x_a P_{beam}$ and $x_b P_{beam}$ of the incident partons :

$$M^2 = x_a x_b s = \hat{s} \tag{7a}$$

$$P_L = (x_a - x_b) P_{beam}. \tag{7b}$$

The transformation to the c.m.s. of the three jets is made using a longitudinal Lorentz boost of velocity $\beta^* = P_L/(P^2_L + M^2)^{1/2}$. In this new system the jet momenta $\vec{p}_i^{\,*}$ obey the relations

$$\Sigma \vec{p}_i^{\,*} = 0, \tag{8a}$$

$$\Sigma p_i^* = M. \tag{8b}$$

After boosting to the centre of mass of the jet system, the leading jets are arranged in order of decreasing p_i^*. The three-jet system can now be described in terms of six variables, three defining the orientation of the plane containing the three-jet system in space, and three defining the configuration of the jets within this plane. Each of these six variables will be investigated. In order to emphasize those features peculiar to QCD, the distributions will be compared with the predictions of the model described in the previous section, as well as with a phase space model obtained by setting the Q_n^{ij} in Equation (4) equal to one. For the purposes of this section, we will concentrate on the shapes of the distributions, leaving the discussion of their normalization to the next Section.

We first define three angles which describe the orientation of the three c.m.s. momenta $\vec{p}_i^{\,*}$. The direction of the leading jet, $\vec{p}_1^{\,*}$, relative to the beam is characterized by two angles : the azimuthal angle ϕ^* and the polar angle θ^*, which are defined using the prescription of Ref. [27]. An additional angle, ψ^*, characterizes the orientation of the remaining two jets. It is defined to be the angle between the plane containing the three jet momenta and the plane containing $\vec{p}_1^{\,*}$ and the beam direction :

$$\cos\psi^* = (\vec{P}_{beam} \times \vec{p}_1^{\,*}) \cdot (\vec{p}_2^{\,*} \times \vec{p}_3^{\,*}) \,/\, [|\vec{P}_{beam} \times \vec{p}_1^{\,*}| \cdot |\vec{p}_2^{\,*} \times \vec{p}_3^{\,*}|] \tag{9}$$

The distribution of the azimuthal angle ϕ^* is found to be consistent with expectations based on the assumption that the beams are unpolarized.

The distribution of $\cos\theta^*$ is shown in Figure 4. This distribution has been corrected for acceptance effects using a two step procedure. First, each event is weighted to account for the limited ψ^* acceptance associated with the presence of a third jet. This correction is calculated by rotating the event around the axis of the leading jet (rotating in ψ^*) and finding the probability that such an event was observed. This correction is typically a factor of 1.2 and is never larger than 1.7. After this correction has been applied, the procedure used in Ref. [4] for two-jet events can be used to account for the limited $\cos\theta^*$ acceptance of the detector as a function of the longitudinal momentum of the jet system. Figure 4 compares the resulting distribution with that found for two-jet events [4]. The shapes are very similar, and are characteristic of vector gluon exchange. A comparison is made both with QCD at the parton level and with the full QCD model of Section 3, in order to ensure that the correction procedure used here is accurate. The curve in Figure 4 shows the parton level calculation of the cross-section for the $gg \rightarrow ggg$ sub-process, computed using Equation (4) and the transverse momentum and angular separation cut-offs described in the preceding section. The curves for the other sub-processes are not significantly different, and therefore the various contributions cannot be experimentally untangled. The overall agreement with QCD is very good, providing a clear test of the underlying dynamics.

The distribution for the angle ψ^* is expected to peak in the regions near 0 and π, corresponding to the case where one of the jets is close to the incident beam direction, due to initial state bremsstrahlung. The limited rapidity coverage of the UA2 detector restricts us to an event sample in which none of the three jets are very close to the beam direction. This means that the expected enhancement is very small. A careful comparison between the data and the distribution of events which would be produced by a phase space model gives evidence for such an enhancement, but the effect is small, and depends on the particular fragmentation model used.

The remaining three variables depend on the internal configuration of the three-jet system, independent of its orientation. The qualitative features can be seen in a Dalitz plot, constructed by defining scaled variables using the two-body masses m_{ij} :

$$x_{ij} = m_{ij}^2 / \hat{s} \qquad (10)$$

Figure 5 shows the distribution of x_{12} versus x_{23}. If the events were distributed according to a phase space density, the population would be uniform across the plot (ignoring acceptance effects). Instead, there is an increased density in the region of small x_{23} (corresponding to final state bremsstrahlung of a soft third jet) compared to that of large x_{23} (corresponding to equal sharing of energy among the three jets). The absence of events near $x_{12} = 1$ and $x_{23} = 0$ is a result of the event selection criteria (1) and of the two-jet angular resolving power. The projections of the Dalitz plot are also shown. They are compared with the QCD and the phase space models. The QCD model agrees well with the data, and there is a large excess of events above the phase space curve in the region of small x_{23}.

The three variables used to give a complete description of the internal configuration are discussed below. The first variable is ω_{23}^*, defined to be the angle between $\vec{p}_2^{\,*}$ and $\vec{p}_3^{\,*}$ It is expected to peak at small values, compatible with the angular resolving power of the detector, due to the contribution of final state bremsstrahlung. The distribution of $\cos\omega_{23}^*$ is shown in Figure 6a. As for the Dalitz plot, a QCD curve and a phase space curve are superimposed over the data. The expected enhancement with respect to the phase space curve is clearly seen. The agreement with QCD is apparent, with the cut-off near $\cos\omega_{23}^* = 0.8$ arising from the 30° resolving power of the clustering algorithm. We do not attempt to make a QCD comparison at smaller angles because the results are sensitive to how well the fragmentation model can reproduce the jet angular resolution shown in Figure 1.

The next variable is p_{out}, defined to be the common magnitude of the components of $\vec{p}_2^{\,*}$ and $\vec{p}_3^{\,*}$ in the direction transverse to $\vec{p}_1^{\,*}$. The distribution of p_{out} is shown in Figure 6b. It peaks at small values, corresponding to narrow $(\vec{p}_2^{\,*}, \vec{p}_3^{\,*})$ pairs, like ω_{23}, but also contains information about the momenta of the softer jets. The histogram represents the prediction of the QCD model, ignoring the small p_{out} region which is sensitive to fragmentation effects. The agreement between the data and the model is quite good.

The last variable to be discussed is the angle ζ, defined to be :

$$\cos\zeta = (p_2^{\,*} - p_3^{\,*})/p_1^{\,*}. \qquad (11)$$

This angle [28] describes the asymmetry of the energy found in the softer two jets. Equivalently, in the rest frame of the $(\vec{p}_2, \vec{p}_3)$ pair, ζ measures the angle between $\vec{p}_1$ and $\vec{p}_3 = -\vec{p}_2$. However, the cuts given by Equation (1) introduce a bias in the event selection which significantly distorts the $\cos\zeta$ distribution. To eliminate this bias, we have studied a smaller sample of three-jet events which have a three-jet mass greater than 85 GeV and lie inside a region of the Dalitz plot given by $0.04 \leq x_{23} \leq 0.16$. The $\cos\zeta$ distribution for the restricted sample is shown in Figure 6c. This distribution has been corrected for acceptance effects using a weight calculated by rotating the event around the leading jet axis, as was done previously for $\cos\theta^*$. The resulting correction is small, typically a factor of 1.1 The data have been compared both with QCD at the parton level and with the full QCD model. The curve in Figure 6c shows the same parton level calculation which was described previously for the $\cos\theta^*$ distribution.

For the three-jet events observed in e^+e^- annihilation, the distribution of $\cos\zeta$ is characteristic of gluon bremsstrahlung off of a $q\bar{q}$ pair, and provides a test of the the spin of the gluon. In this experiment, where many different subprocesses contribute to three-jet production, the $\cos\zeta$ distribution remains a sensitive probe of the underlying dynamics. The observed agreement between the data and the QCD model prediction is a further test of the validity of QCD.

5. THE STRONG COUPLING CONSTANT AND THE THREE−JET TO TWO−JET RATIO

In the preceding Section we used selection criteria which allowed us to display the dominant features of the three-jet data sample. In particular, loose cuts were used on the jet transverse momenta and on the opening angle of jet pairs (Figure 1) to study the effect of bremsstrahlung. In this way, we have shown that the QCD model introduced in Section 3 gives a good description of the shapes of the three-jet distributions. We know from former studies [1-6] that it also provides a good description of the two-jet sample. In the present Section, we want to pursue a more quantitative comparison with the QCD model. To this end, we measure the quantity $\alpha_s\, K_3/K_2$ by adjusting α_s in the QCD model until the theoretical value of the ratio between the three-jet cross-section and the two-jet cross-section (R_{QCD}) is equal to its experimental value, R_{exp}.

There are several sources of systematic error associated with this measurement which can be reduced by applying stricter event selection criteria. We want to avoid those regions of phase space where either two of the partons are separated by a small angle, or one of the partons is soft. These regions are sensitive in particular to fragmentation effects, such as the energy scale (the fraction of the original parton energy measured by the jet algorithm) and the angular resolving power (see Figure 1). For this reason, we redefine the two-jet and three-jet data samples using two additional criteria :

i. the clustering algorithm defined in Section 2 is followed by an additional step in which secondary cluster pairs, having an opening angle smaller than 50° and a transverse energy in excess of 5 GeV, are merged into a single cluster (Figure 1). This merging results in an effective resolving power exceeding 99% above 50° and cutting off sharply below this angle;

ii. the 10 GeV threshold used in (1b) and (2b) is replaced by a 15 GeV threshold to further reduce the contamination from spectator particles. The 8 GeV transverse momentum cut-off used in the QCD model generation is accordingly replaced by a 12 GeV cut-off.

The new selection criteria are summarized in Table 1. They retain 14635 two-jet and 2596 three-jet events. The experimental value R_{exp} is simply calculated as the ratio between these two numbers. Events containing more than 2 (3) such jets are not included in the two-(three-) jet sample. This procedure gives a value $R_{exp} = 0.177 \pm 0.004$.

The normalized distributions of the longitudinal momentum P_L and of the invariant mass M are shown in Figure 7 for the data and the Monte Carlo samples. As a result of Equations (7a) and (7b), they are largely controlled by the x-dependence of the structure functions, which have been obtained from two-jet data. The agreement between the data and the QCD model prediction demonstrates that the same structure functions describe the three-jet data.

The selection criteria of Table 1 are also applied to the Monte Carlo event samples. The values for the cut-offs used in the QCD model at parton level are required to define $\alpha_s K_3/K_2$. They are low enough, when compared to the corresponding event selection cuts applied at cluster level, so that events generated with lower cut-offs would not pass the selection cuts. These cut-offs are applied to all outgoing partons, whether or not they are inside the acceptance. The value of R_{QCD} is then the ratio between two cross-sections, σ_3^{QCD} and σ_2^{QCD}. We include in σ_3^{QCD} those events from σ_3^{LO} and σ_4^{LO} which have three and only three jets obeying the selection criteria. Similarly, σ_2^{QCD} contains events generated from σ_2^{LO} and σ_3^{LO} which have two and only two jets obeying the selection criteria. The relative contributions to σ_3^{QCD} from σ_4^{LO} and to σ_2^{QCD} from σ_3^{LO} are respectively 21% and 16%. Higher order contributions, such as from σ_5^{LO} to σ_3^{QCD} and from σ_4^{LO} to σ_2^{QCD} are ignored. Lacking even an estimate of the former we prefer not to correct for the latter, as we expect their contributions to R_{QCD} to partially cancel and result in a small global effect.

By varying α_s in the QCD model, we find that the value of the strong coupling constant that makes R_{QCD} equal to R_{exp} is

$$\alpha_s K_3/K_2 = 0.23 \pm 0.01. \qquad (12a)$$

The effects of the dependence of α_s on q^2 (Equation 6) are displayed in Figure 8, which shows the values of $\alpha_s K_3/K_2$ in different bins of the multi-jet mass M. The q^2-range covered by the data sample is from ~600 to 10,000 GeV^2, with the average $q^2 \sim 1700$ GeV^2. The curve in Figure 8, obtained by computing α_s for an average q^2 calculated for each mass bin in the Figure, shows the expected $\pm 7\%$ variation of α_s over this mass range. The data are in agreement with the curve, but show no significant deviation from a constant value.

Several sources of systematic uncertainties affect our evaluation of the strong coupling constant (12a). We now consider each of these in turn and evaluate their contributions to the error on $\alpha_s K_3/K_2$.

i. The integrated luminosity cancels in the evaluation of R_{exp} and does not contribute to the uncertainty on α_s.

ii. The form chosen for the fragmentation functions is the major source of uncertainty when measuring α_s in e^+e^- annihilations [13]. In the higher energy range of the present experiment, there is virtually no ambiguity in distinguishing between two-jet and three-jet configurations. Instead, the main consequence of using different fragmentation functions is to modify the fraction of the original parton energy which is collected in the corresponding calorimeter cluster. This affects the three-jet sample, which often contains a relatively soft third jet near the

15 GeV transverse momentum cut, more than the two-jet sample. Changes in the fragmentation model compatible with the observed cluster radius distribution (and with the upper bound placed by $\tilde{E}_T$ on the jet energy not contained in the leading clusters, see iii) below), produce variations of α_s which do not exceed $(\Delta\alpha_s/\alpha_s) \simeq \pm 10\%$.

iii. The spectator scattering contribution is simulated by superimposing a minimum bias event onto each generated hard collision. However, we know [2,16] that the value of $\tilde{E}_T$ is, on average, twice as high for hard collisions as for minimum bias events. Part of the difference can be accounted for by particles directly associated with the hard collision. Nevertheless, we have studied the effect of doubling the transverse energy carried by the underlying event. This was done by superimposing onto each generated hard collision either two independent minimum bias events or a single event modified by doubling each cell energy. From this study we evaluate an uncertainty on α_s, $(\Delta\alpha_s/\alpha_s) = \pm 10\%$. In addition, we quote the final value of α_s for an underlying event configuration carrying on average 1.5 ± 0.5 times the transverse energy of a minimum bias event. This value is in agreement with the contribution to the underlying event coming from our fragmentation model, and the uncertainty attached to it is taken into account in the uncertainty on α_s quoted above.

iv. Uncertainties in the structure functions may affect the α_s measurement to the extent that the quark to gluon ratio may be modified. Because of the higher colour charge of gluons, a relative increase of the gluon content results in a larger value of R_{QCD}, and consequently in a lower value of α_s. We evaluate this effect by varying the gluon to quark ratio in the structure functions (see Equation 5) within limits compatible with the measured two-jet cross-section [4,6] with the result that $(\Delta\alpha_s/\alpha_s) = \pm 7\%$.

v. Systematic uncertainties in the energy response of the UA2 central calorimeter (both in shape and in absolute calibration) have been considered in detail in previous publications [2,3,6,14]. Their contributions to R_{exp} partially cancel since they affect both the two-jet and the three-jet samples. They introduce an uncertainty on the α_s measurement of $(\Delta\alpha_s/\alpha_s) = \pm 3\%$.

vi. The contribution to R_{QCD} from σ_4^{LO} is important, of the order of 21%. As mentioned earlier, σ_4^{LO} is normalized to the number of events containing four observed jets. However, several additional checks have been made. The bremsstrahlung model does describe the configurations of the small number of observed four-jet events. A more complete check was performed by generating three-jet events, using the technique described in Section 3, from the σ_2^{LO} calculation and comparing them with events from the full σ_3^{LO} calculation. The results are in agreement. We estimate from these observations an uncertainty of $\pm$ 40% on the absolute scale of σ_4^{LO} which appears in the α_s measurement as an error $(\Delta\alpha_s/\alpha_s) = \pm 8\%$.

vii. Our measurement of α_s is, in principle, independent of the criteria (Table 1) used to select the jet samples, as long as these selection criteria are compatible with the cut-offs used in the model. We have re-evaluated α_s varying the cuts of Table 1 and we have observed no significant effect, even for cuts retaining only one half of the event samples. Moreover, from the comparison between the P_T distributions of the two-jet and three-jet samples (Figure 3), we infer an upper limit $(\Delta\alpha_s/\alpha_s) < 4\%$ on the uncertainty resulting from the absence of explicit P_T dependence in the QCD model.

A summary of the evaluation of α_s K_3/K_2 and of the attached uncertainties is given in Table 2. Some effects are accounted for in several of the systematic uncertainties described above. We conservatively ignore this double counting and retain as a global systematic uncertainty the number obtained by adding all individual contributions, ii) to vii), in quadrature. The result is

$$\alpha_s\, K_3/K_2 = 0.23 \pm 0.01 \pm 0.04 \qquad (12b)$$

where the second error represents the systematic uncertainty.

Finally, we note that our choice of q^2 in the scaling violation factors is somewhat arbitrary. We mentioned earlier that another choice would not affect α_s, but would only modify Λ, as long as the two-jet and three-jet samples are treated equally. However, it is possible to choose q^2 definitions which alter the average q^2 of the two-jet sample with respect to that of the three-jet sample. We have considered a concrete example by replacing our choice, $\sqrt{q^2} = \text{Max}\,(p_T^i)$, by $\sqrt{q^2} = <p_T^i>$, thereby reducing the three-jet $<q^2>$ with respect to the two-jet $<q^2>$. This change decreases the mean value of q^2 for the three-jet analysis while leaving the mean value of q^2 for the two-jet analysis unchanged. The result is to increase only the value of α_s that appears in the calculation of σ_3^{LO}, typically by 8%, and hence to increase the value of R_{QCD}. As a consequence, the measured value of $\alpha_s\, K_3/K_2$ decreases by 25%.

6. CONCLUSIONS

We have presented a detailed study of final states containing three hard jets observed in $\bar{p}p$ interactions at $\sqrt{s} = 630$ GeV. The configurations of these events in the centre of mass of the jet system have been examined and compared to a QCD model including all lowest order sub-processes. Two general features emerge from these comparisons. First, the orientation of the event in space provides information about the scattering processes involved. In particular, the distribution of the angle of the leading jet relative to the beam direction, $\cos\theta^*$, agrees well with the QCD model and also with the distribution observed in previous studies of two-jet events [4]. This behavior is characteristic of Rutherford-like scattering (t-channel exchange of a vector gluon). Second, the internal configuration of the three-jet system provides clear evidence for the presence of bremsstrahlung processes. This is apparent in the Dalitz plot as an enhancement at small x_{23} (the scaled squared mass of the two softest jets) as well as in the $\cos\omega_{23}^*$ (the angle between the softest jets) plot. In both cases, the observed distributions deviate significantly from phase space. This quantitative agreement of all of the measured distributions with the QCD model provides further support for QCD as a theory of strong interactions.

We have put particular emphasis on a quantitative evaluation of the strong coupling constant α_s. Until recently this measurement was dominated by e^+e^- annihilation experiments [13]. Such experiments are ultimately expected to reach the highest accuracy, since the quark-gluon vertex is decoupled from the primary electroweak annihilation process. In practice, however, these measurements have encountered a number of difficulties [30] associated with the relatively low values of $\sqrt{\hat{s}}$ (< 35 GeV) at which they have been performed. The values of α_s measured by these experiments are in the range $0.12 - 0.16$ for independent jet fragmentation models [31] and $0.14 - 0.23$ for string fragmentation models [32]. The above values are obtained using a QCD model which includes second order contributions in α_s, where the non-leading corrections typically reduce the first order value by 25%. Alternative α_s measurements, obtained using a technique based on the measurement of the total cross-section for $e^+e^- \to$ hadrons [33], are insensitive to fragmentation effects, but are limited by other sources of systematic error.

The present experiment probes much higher values of $\sqrt{\hat{s}}$, ≈ 90 GeV on average, thus dealing with better separated jets in the final state. However, it has to face other important sources of uncertainties, specific to hadron collisions. In particular, the presence of spectator fragments limits the size of the cone around the jet axis which can be used to measure the jet energy. The fraction of the initial parton energy contained in these cones depends on the fragmentation model. In addition, the very large number of relevant subprocesses has, for the time being, precluded reliable calculations of higher order contributions.

We have attempted to minimize the impact of these problems by reducing our data to a form amenable to direct confrontation with theoretical models and by unfolding the instrumental effects to the best of our knowledge. We have defined jets by introducing cut-offs at the parton level, and we have dealt with exclusive topological cross-sections in order to quote a result which can be more reliably compared to leading order QCD calculations.

Our final result (12b) is numerically very close to that of the UA1 Collaboration [12], obtained using the same q^2-scale for two-jet and three-jet events,

$$\alpha_s \, K_3/K_2 = 0.23 \pm 0.02 \pm 0.04. \qquad (13)$$

However, several differences between the definitions used by the two Collaborations can be expected to have significant effects on α_s. The definition of q^2-scale used by UA1 in deriving the result shown in Equation (13) is different than the one used here. The UA1 definition corresponds to average q^2 values which are identical when expressed as fractions of the multi-jet mass: $<q_2/M_2> = <q_3/M_3> = 0.45$, where $q_{2,3}$ is $\sqrt{q^2}$ for the two and three jet samples and $M_{2,3}$ is the mass for these samples. The definition used in the analysis presented here, corresponding to the transverse momentum of the leading jet, gives a softer q^2 distribution for the three jet sample: $<q_2/M_2> = 0.48$ and $<q_3/M_3> = 0.41$. In addition, the UA1 α_s value is obtained using inclusive topological cross-sections and corresponds to different values for the cut-offs than those used here.

When compared with the results from e^+e^- experiments, even the extrapolation of the string fragmentation values to the Collider region give a result that is typically 30% lower than the values of $\alpha_s \, K_3/K_2$ measured by UA1 and UA2. This discrepancy (which does not exceed the quoted uncertainties by very much) may be due to the effect of higher order corrections to K_3 and K_2, or to a different q^2 scale in two-jet and three-jet processes. The latter point of view has been advocated by UA1 [12] and they have observed that a comparison of event samples with q^2-scales that satisfy the intuitive rule $<q_3> \sim 2/3 <q_2>$ reduces their value for $\alpha_s \, K_3/K_2$ from 0.22 to 0.16. This ambiguity in the choice of q^2-scale cannot be resolved until the higher order QCD corrections are computed. Since these have not yet been calculated, we choose to quote our result for the assumption that the definition of the q^2-scale using the transverse momentum of the leading jet is appropriate for both the two-jet and three-jet samples.

The above discussion indicates that conceptual rather than instrumental limitations preclude a more accurate and more reliable measurement of α_s. Calculations of K_3/K_2 and a better understanding of the relevant q^2-scales are needed to improve the determination of α_s by the present method.

ACKNOWLEDGEMENTS

This experiment would have been impossible without the very successful operation of the CERN $\bar{p}p$ Collider whose staffs and coordinators we gratefully acknowledge for their collective effort.

We deeply thank the technical staffs of the institutes collaborating in UA2 for their important contributions to maintain and improve the performance of the detector.

We are grateful to the UA4 Collaboration for providing the signals from their small-angle scintillator arrays and to the UA5 Collaboration for the loan of scintillator hodoscopes.

We have enjoyed many fruitful discussions with colleagues from the theory departments. In particular, we thank S. Ellis, Z. Kunszt (who allowed us the use of his QCD calculations in Monte Carlo form), and J. Stirling.

Financial support from the Schweizerischer Nationalfonds zur Förderung der Wissenschaftlichen Forschung to the Bern group, from the Danish Natural Science Research Council to the Niels Bohr Institute group, from the Bundesministerium für Forschung und Technologie to the Heidelberg group, from the Institut National de Physique Nucléaire et de Physique des Particules to the Orsay group, from the Istituto Nazionale di Fisica Nucleare to the Pavia, Perugia and Pisa groups and from the Institut de Recherche Fondamentale (CEA) to the Saclay group are acknowledged.

REFERENCES AND FOOTNOTES

1. UA2, M. Banner et al., Phys. Lett. **118B** (1982) 203.
2. UA2, P. Bagnaia et al., Z. Phys. **C20** (1983) 117.
3. UA2, P. Bagnaia et al., Phys. Lett. **138B** (1984) 430.
4. UA2, P. Bagnaia et al., Phys. Lett. **144B** (1984) 283.
5. UA2, P. Bagnaia et al., Phys. Lett. **144B** (1984) 291.
6. UA2, J.A. Appel et al., Phys. Lett. **160B** (1985) 349.
7. UA1, G. Arnison et al., Phys. Lett. **123B** (1983) 115.
8. UA1, G. Arnison et al., Phys. Lett. **132B** (1983) 214.
9. UA1, G. Arnison et al., Phys. Lett. **132B** (1983) 223.
10. UA1, G. Arnison et al., Phys. Lett. **136B** (1984) 294.
11. UA1, G. Arnison et al., Phys. Lett. **147B** (1984) 222.
12. UA1, G. Arnison et al., Phys. Lett. **158B** (1985) 494.
13. Mark J, B. Adeva et al., Phys. Rev. Lett. **54** (1985) 1750 ;
    JADE, W. Bartel et al., Z. für Phys. **C25** (1984) 231 ;
    CELLO, H.J. Behrend et al., Phys. Lett. **138B** (1984) 311 ;
    TASSO, M. Althoff et al., Z.für Phys. **C26** (1984) 157 ;
    S.L. Wu, Phys. Rep. **107** (1984) 59.
14. A. Beer et al., Nucl. Instr. Meth. **224** (1984) 360.
15. UA4, M. Bozzo et al., Phys. Lett. **147B** (1984) 392.
16. UA2, J.A. Appel et al., Experimental study of the emergence of two-jet dominance in $\bar{p}p$ collisions at $\sqrt{s}$ = 630 GeV, CERN-EP/85-136, 30 August 1985, submitted to Phys. Lett. B.
17. M. Greco, Z. Phys. C **26** (1985) 567.
18. B.L. Combridge, L. Kripfganz and J. Ranft, Phys. Lett. **70B** (1977) 234;
    R. Cutler and D. Sivers, Phys. Rev. **D17** (1978) 196.
19. Z. Kunszt and E. Pietarinen, Nucl. Phys. **B164** (1980) 45 ;
    T. Gottschalk and D. Sivers, Phys. Rev. **D21** (1980) 102 ;
    F.A. Berends et al., Phys. Lett. **118B** (1981) 124.
20. G. Sterman and S. Weinberg, Phys. Rev. Lett. **39** (1977) 1436 ;
    K. Shizuya and S.H.H. Tye, Phys. Rev. Lett. **41** (1978) 787 and Phys. Rev. **D20** (1979) 1101 ;
    M.B. Einhorn and B.G. Weeks, Nucl. Phys. **B146** (1978) 445.

21. B. Cox, Proc. 21st Int. Conf. on High Energy Physics, Paris, 26-31 July 1982, ed. P. Petiau and M. Porneuf, p. C3-140.

22. N.G. Antoniou et al., Phys. Lett. **128B** (1983) 257.

23. CDHS, H. Abramowicz et al., Z. Phys. **C12** (1982) 289, **C13** (1982) 199, **C17** (1983) 283, and private communication from F. Eisele. We have studied the effect of using other structure functions, and found that our conclusions were insensitive to this choice after evolution to the q^2-range of the present experiment. See e.g. CHARM, F. Bergsma et al., Phys. Lett. **153B** (1985) 111.

24. G. Altarelli and G. Parisi, Nucl. Phys. **B126** (1977) 298.

25. R.D. Field and R.P. Feynman, Nucl. Phys. **B136** (1978) 1.

26. T.A. DeGrand, Y.J. Ng, S.H.H. Tye, Phys. Rev. **D16** (1977) 3251 ;
J. Ellis, M.K. Gaillard and G.G. Ross, Nucl. Phys. **B11** (1976) 253.

27. J.C. Collins and D.E. Soper, Phys. Rev. **D16** (1977) 2219.

28. J. Ellis and I. Karliner, Nucl. Phys. **B148** (1979) 141.

29. TASSO, R. Brandelik et al., Phys. Lett. **97B** (1980) 453.

30. T. Sjostrand, Z. Phys. **C26** (1984) 93.

31. P. Hoyer et al., Nucl. Phys. **B161** (1979) 349 ;
A.Ali et al., Phys. Lett. **93B** (1980) 155.

32. B. Andersson et al., Phys. Rep. **97** (1983) 31.

33. B. Naroska, Electro-weak Interference Effects in e^+e^- Interactions, DESY 85-090, August 1985, and References contained therein.

TABLE 1

Selection criteria used in the α_s analysis

	Parton level (Monte Carlo)	Cluster level (Data and Monte Carlo)
Transverse energy of a jet	$E_T > 12$ GeV	$E_T > 15$ GeV
Range of pseudorapidity for jets	$\|\eta\| < 1.05$	$\|\eta\| < 0.80$
Angular separation between jets	$\omega < 40°$	$\omega < 50°$
Transverse energy of the jet system	$\Sigma_J E_T > 60$ GeV	$\Sigma_J E_T > 70$ GeV
Transverse momentum of the jet system	–	$P_T < 20$ GeV

TABLE 2

Results of the α_s analysis

Data samples	
Two-jet events	14635
Three-jet events	2596
Four-jet events	106
Three-jet to two-jet ratios at $\sqrt{s}$ = 630 GeV	
R_{exp}	0.177 ± 0.004
$\alpha_s K_3/K_2$	0.23 ± 0.01
Relative systematic uncertainties $\Delta\alpha_s/\alpha_s$	
Fragmentation	10%
Spectator scattering	10%
Structure functions	7%
Energy response	3%
Four-jet contribution	8%
P_T dependence	4%
Global result	
$\alpha_s K_3/K_2$ = 0.23 ± 0.01 (stat.) ± 0.04 (syst.)	

FIGURE CAPTIONS

1. The fraction F of clusters resolved by the algorithm as a function of the opening angle ω between clusters i and j, for $E_T^i > 30$ GeV and two values of E_T^j : $E_T^j > 10$ GeV (•) and $E_T^j > 30$ GeV (o). The arrow represents the minimum opening angle at which jets are merged using the algorithm described in Section 5.

2. The probability P_ε that an event contains a third cluster having a transverse energy in excess of ε, as a function of $E_T^1 + E_T^2$, the sum of the transverse energies of the two leading clusters, for three values of ε : $\varepsilon > 10$ GeV (•), $\varepsilon > 15$ GeV (o) and $\varepsilon > 20$ GeV (■).

3. The normalized distribution of the transverse momentum P_T of the jet system for two-jet events (o) and three-jet events (•).

4. The distribution of $\cos\theta^*$ (•), the angle of the leading jet with respect to the beam line, normalized to one at $\cos\theta^* = 0$ and corrected for detector and acceptance effects. The full line represents the QCD model prediction discussed in the text. The measured values for two-jet events [4] are also shown (o).

5. The Dalitz plot ($m_{12}^2/\hat{s}$ vs $m_{23}^2/\hat{s}$) for three-jet events. Two sets of curves are superimposed on the projections. The solid histograms represent the QCD model prediction, and the dashed curves represent phase space, including acceptance effects.

6. a. The normalized distribution of $\cos\omega_{23}^*$, the angle between $\vec{p}_2^{\,*}$ and $\vec{p}_3^{\,*}$. The full line is the QCD model prediction, including detector effects, and normalized in the region $\cos\omega_{23}^* \leq 0.8$. The dashed line represents phase space.

   b. The normalized distribution of p_{out}, the common magnitude of the components of $\vec{p}_2^{\,*}$ and $\vec{p}_3^{\,*}$ transverse to $\vec{p}_1^{\,*}$. The full line represents the QCD model prediction, including detector effects.

   c. The distribution of $\cos\zeta$, corrected for detector acceptance and normalized to one at $\cos\zeta = 0$. The full line represents the QCD model prediction discussed in the text.

7. The normalized distributions for the three-jet sample defined in Table 1. The full line is the prediction of the QCD model.

   a. The longitudinal momentum P_L.

   b. The three-jet mass M. The mass distribution for the two jet sample is also shown (o), together with the corresponding QCD model, normalized to the three-jet sample.

8. $\alpha_s K_3/K_2$ evaluated in bins of the mass of the multi-jet system M. The full line shows the final result and the dashed lines indicate the overall statistical and systematic error. The curve represents the variation of α_s predicted by QCD.

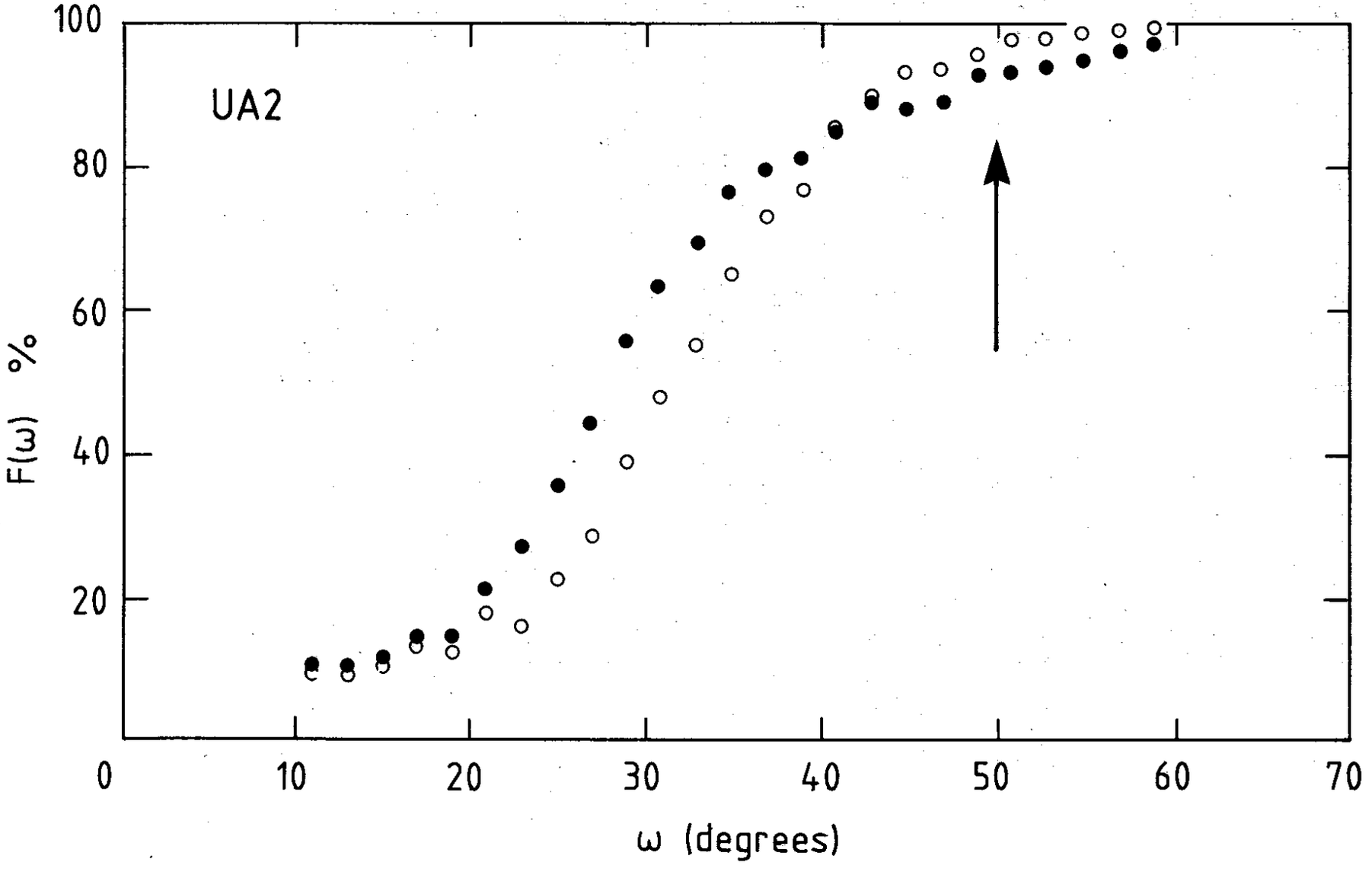

Fig. 1

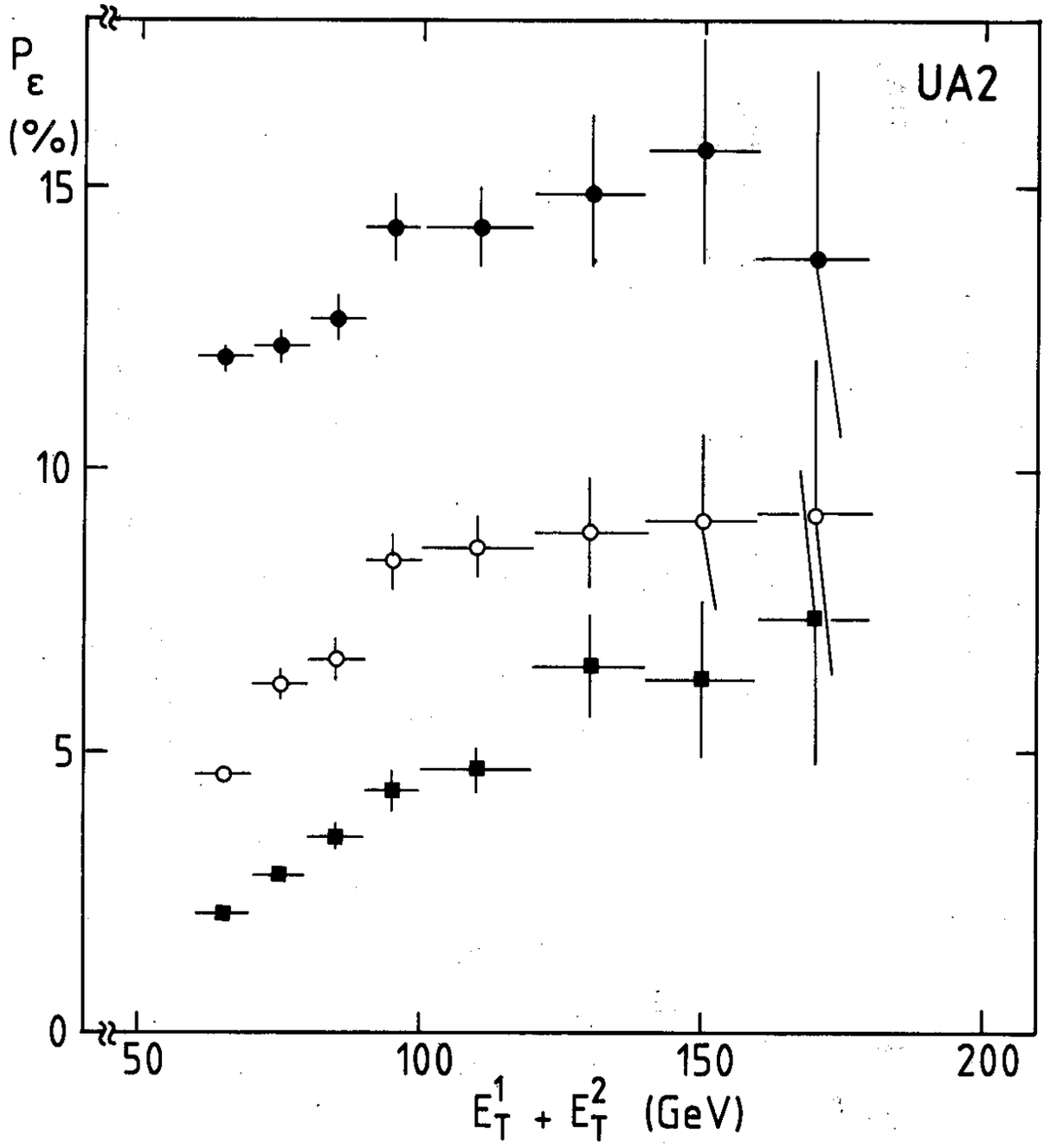

Fig. 2

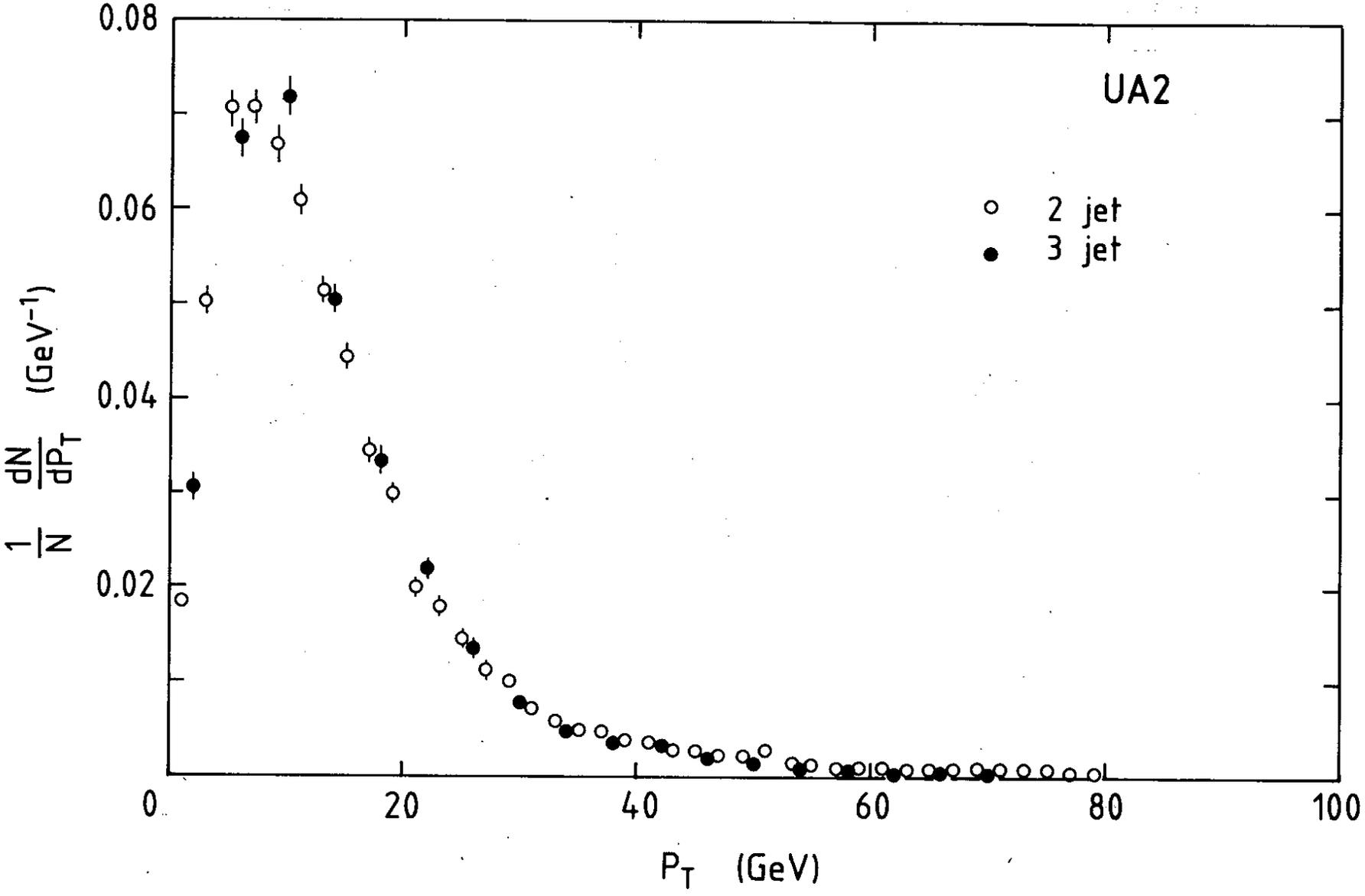
UA2
2 jet
3 jet
0.08
0.06
0.04
0.02
0
20
40
60
80
100
$\frac{1}{N}\frac{dN}{dP_T}$ (GeV^{-1})
P_T (GeV)

Fig. 3

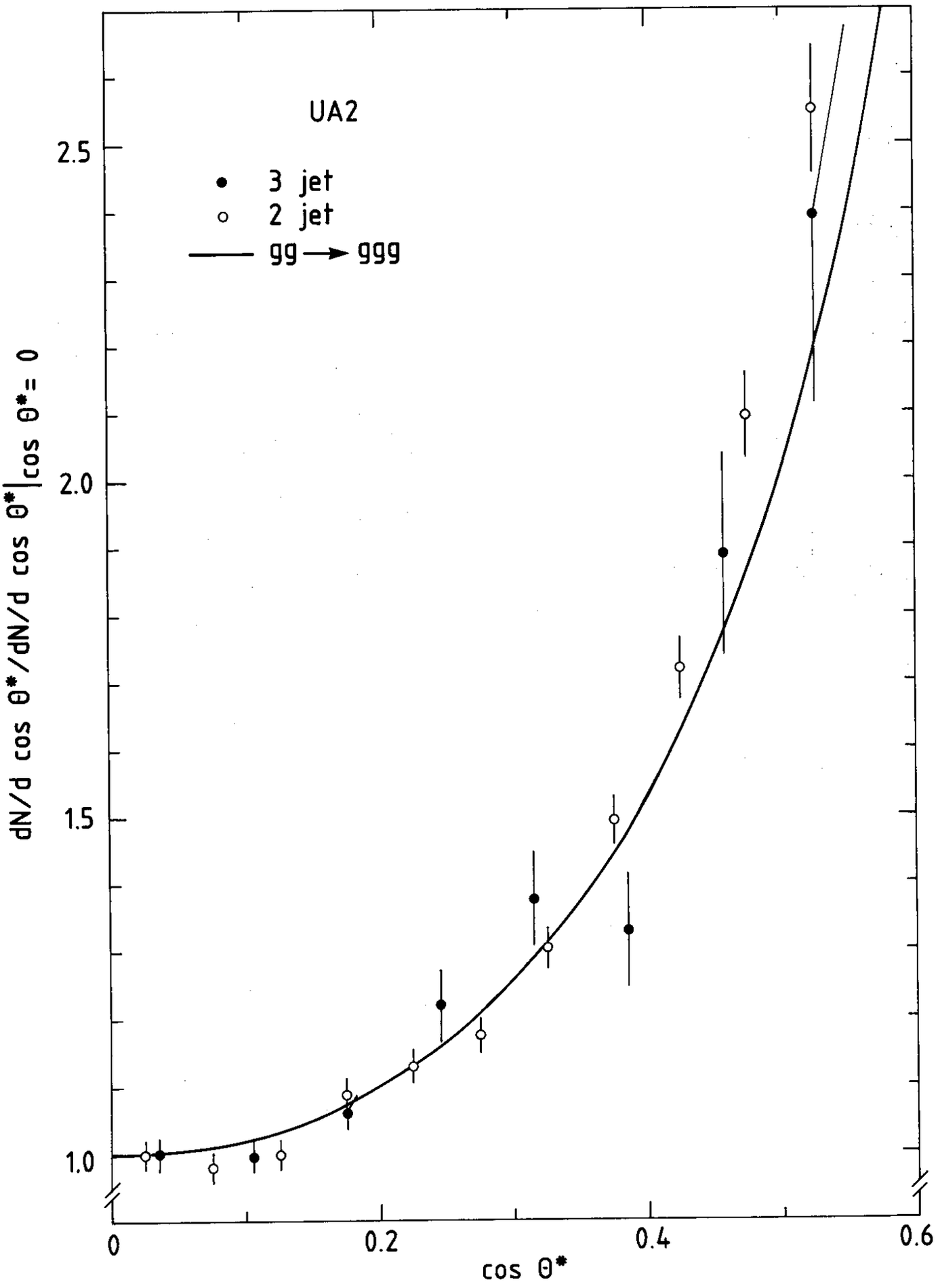
UA2
3 jet
2 jet
gg → ggg
dN/d cos θ* / dN/d cos θ*|cos θ*= 0
2.5
2.0
1.5
1.0
0
0.2
0.4
0.6
cos θ*

Fig. 4

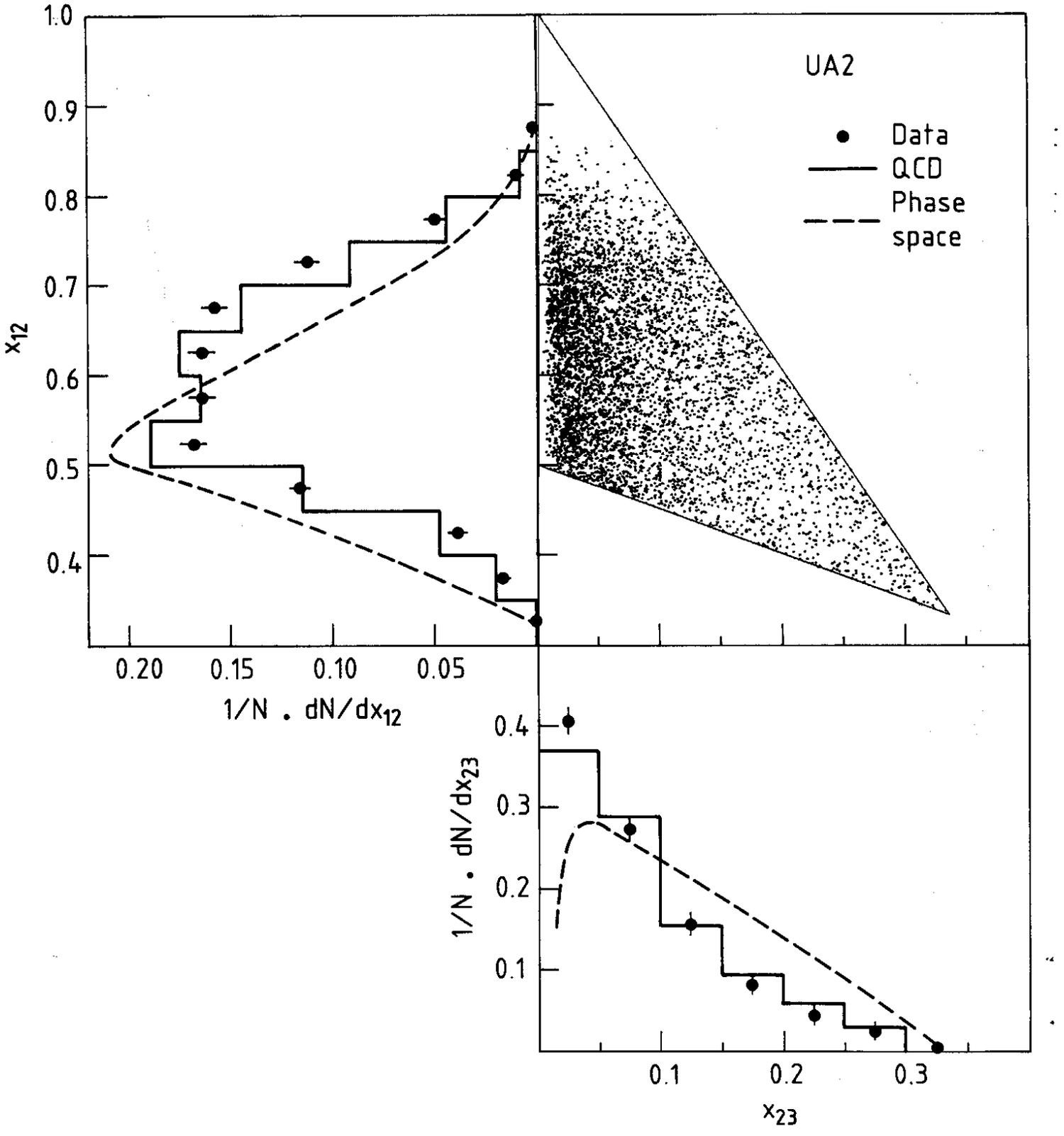
UA2
Data
QCD
Phase space
1.0
0.9
0.8
0.7
0.6
0.5
0.4
x_{12}
0.20
0.15
0.10
0.05
$1/N \cdot dN/dx_{12}$
0.4
0.3
0.2
0.1
$1/N \cdot dN/dx_{23}$
0.1
0.2
0.3
x_{23}

Fig. 5

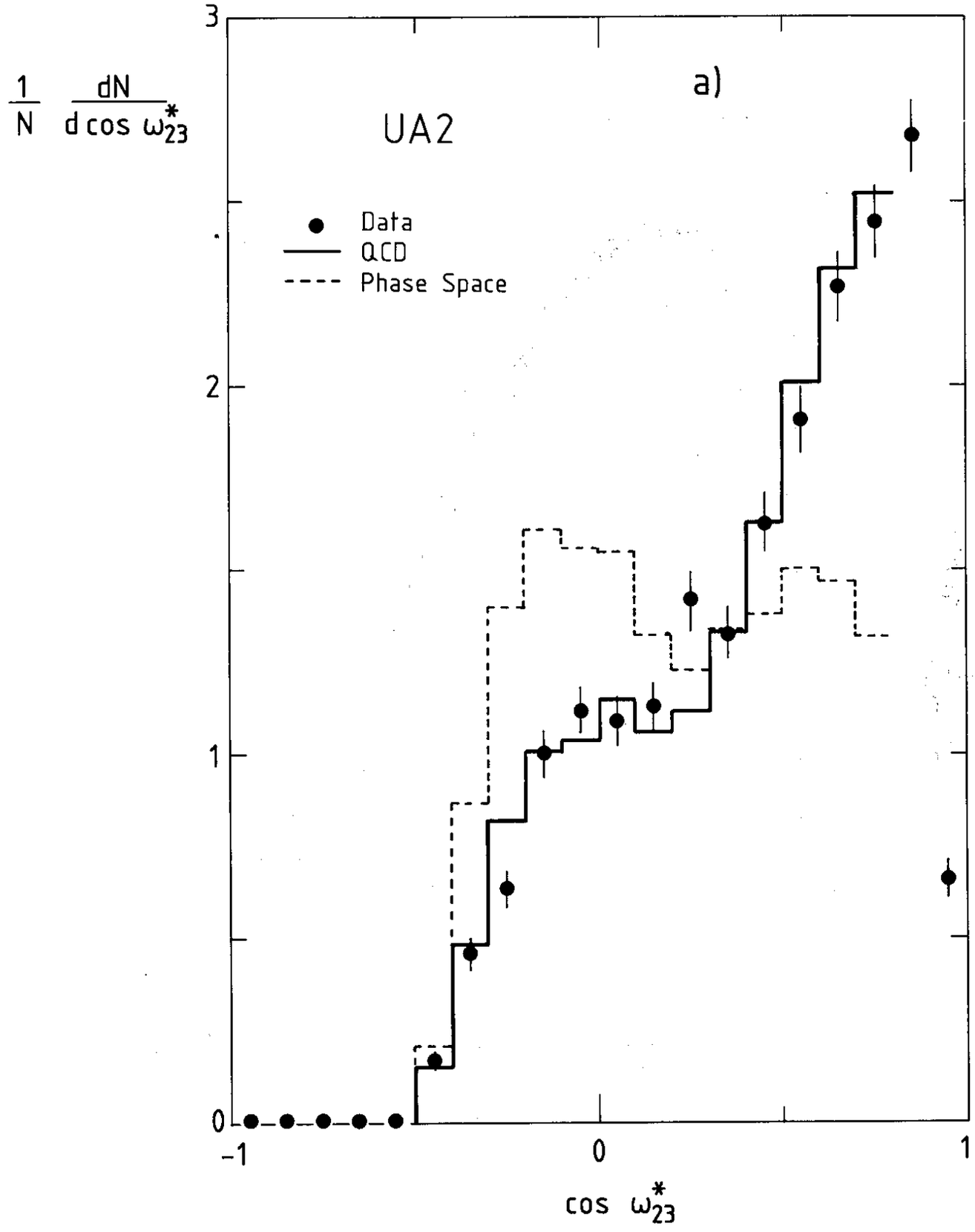
$\frac{1}{N}\frac{dN}{d\cos\omega^*_{23}}$
a)
UA2
Data
QCD
Phase Space
3
2
1
0
-1
0
1
$\cos\omega^*_{23}$

Fig. 6a

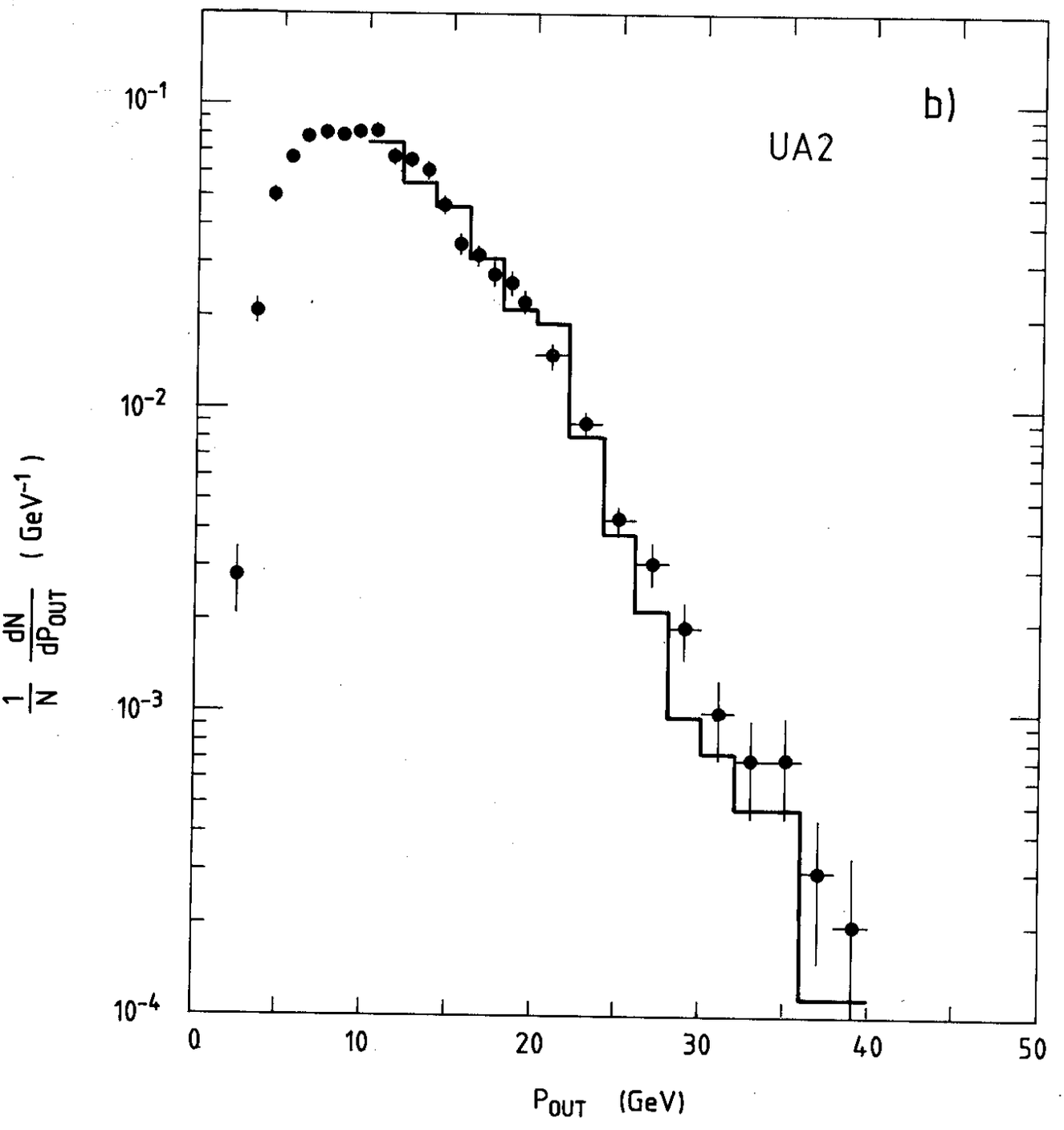
b)
UA2
10^{-1}
10^{-2}
10^{-3}
10^{-4}
$\frac{1}{N}\frac{dN}{dP_{OUT}}$ (GeV^{-1})
0
10
20
30
40
50
P_{OUT} (GeV)

Fig. 6b

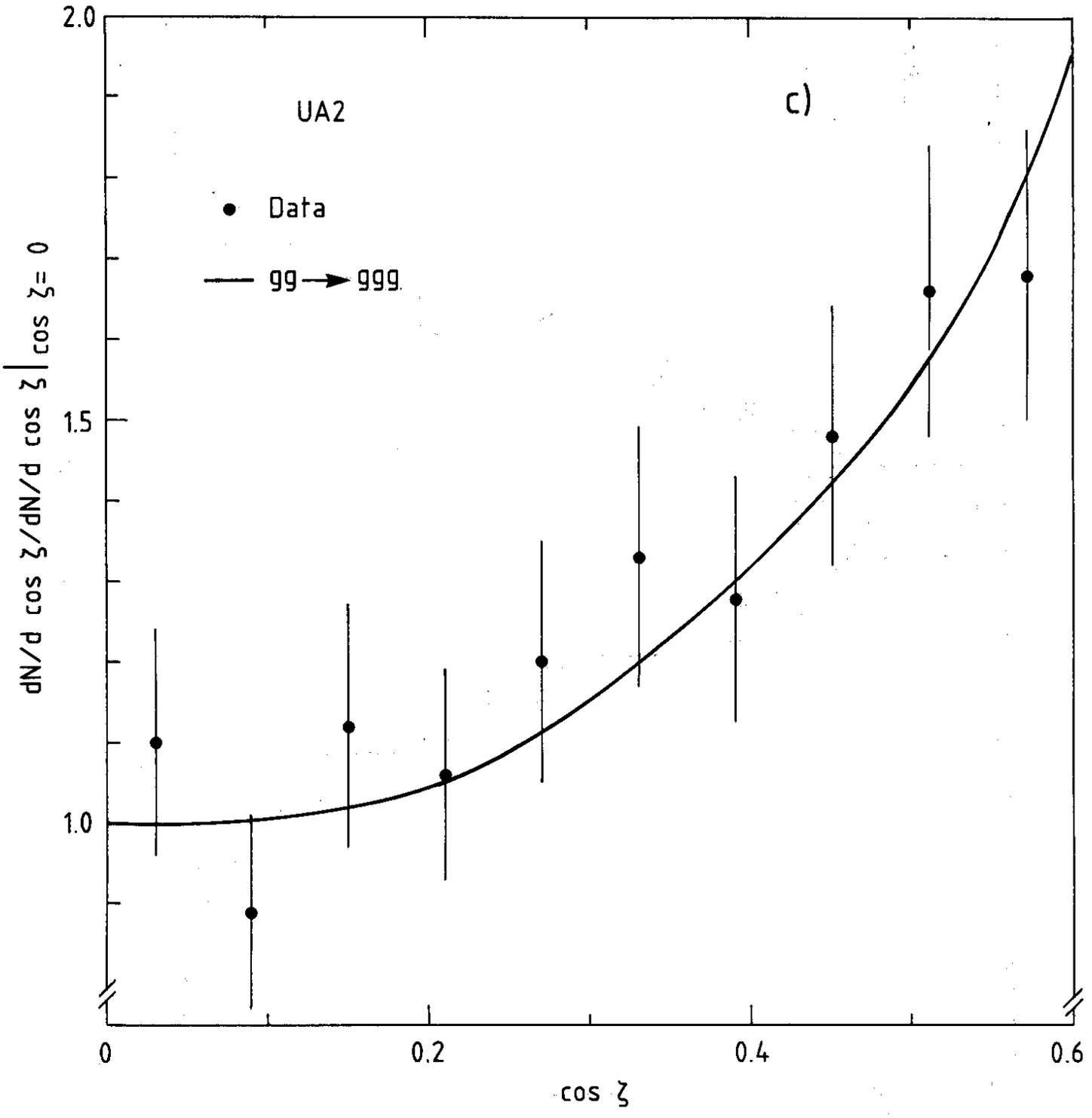

Fig. 6c

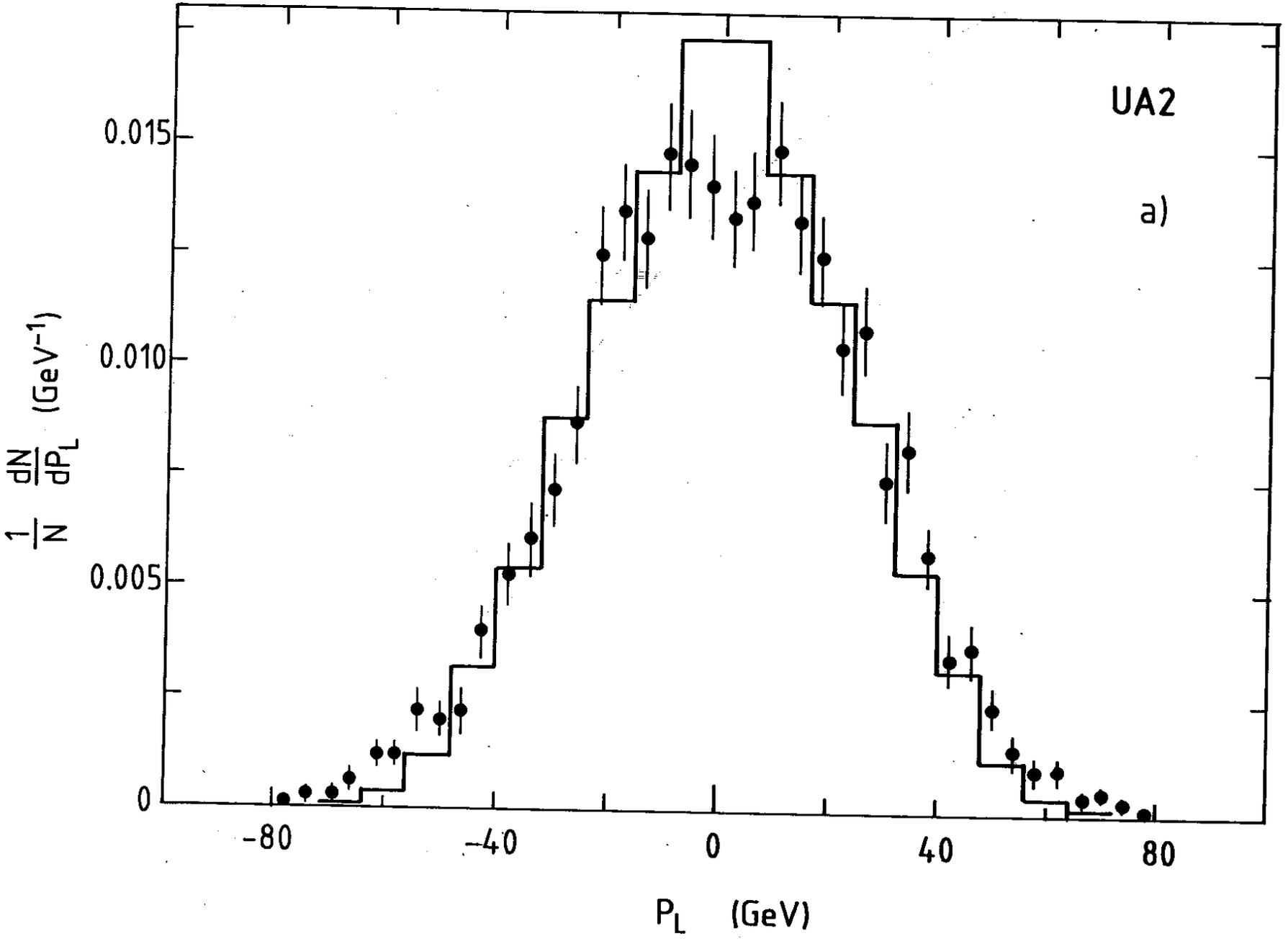
UA2
a)
0.015
0.010
0.005
0
$\frac{1}{N}\frac{dN}{dP_L}$ (GeV^{-1})
-80
-40
0
40
80
P_L (GeV)

Fig. 7a

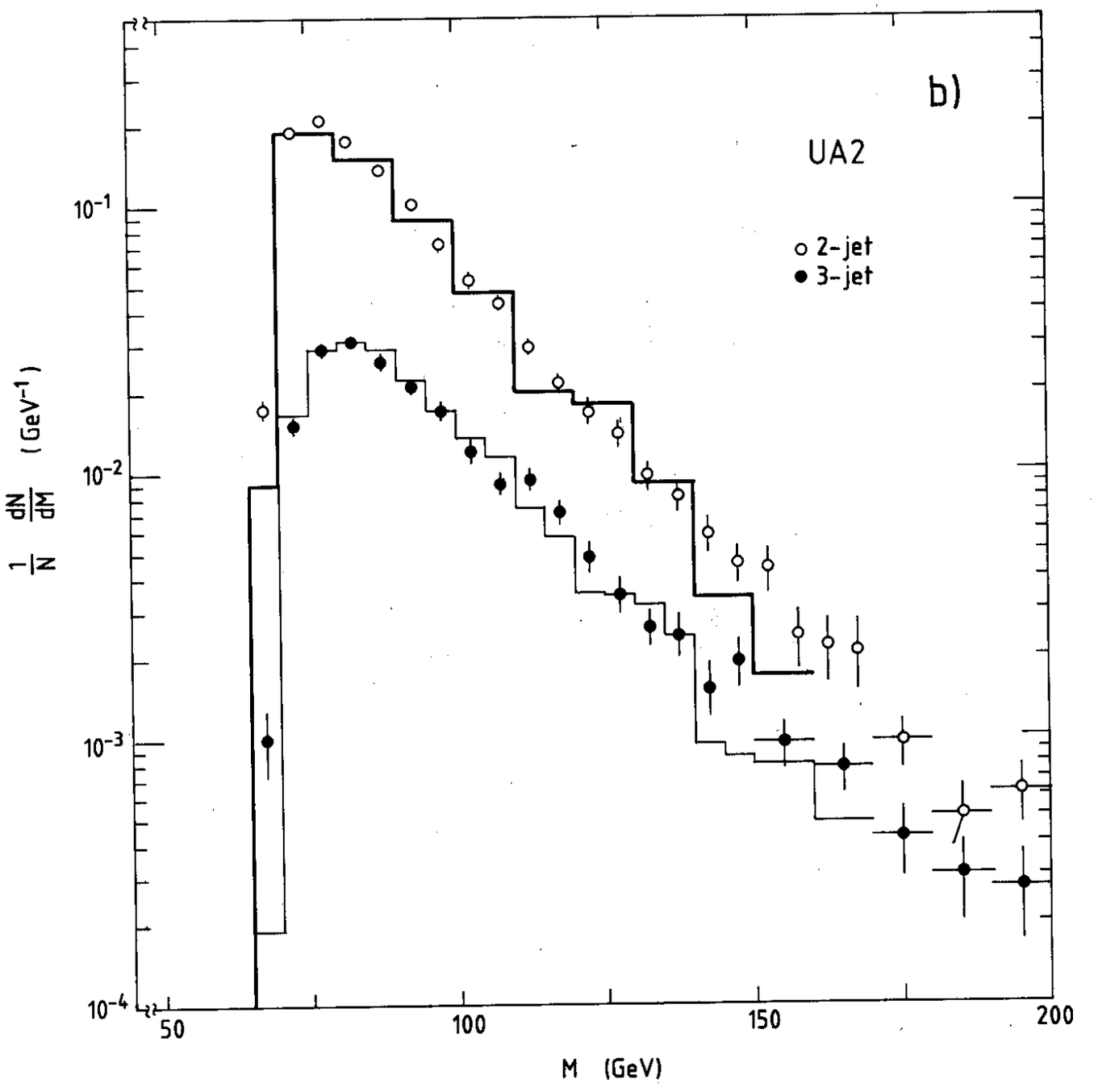
b)
UA2
o 2-jet
• 3-jet
10^{-1}
10^{-2}
10^{-3}
10^{-4}
$\frac{1}{N}\frac{dN}{dM}$ (GeV^{-1})
50
100
150
200
M (GeV)

Fig. 7b

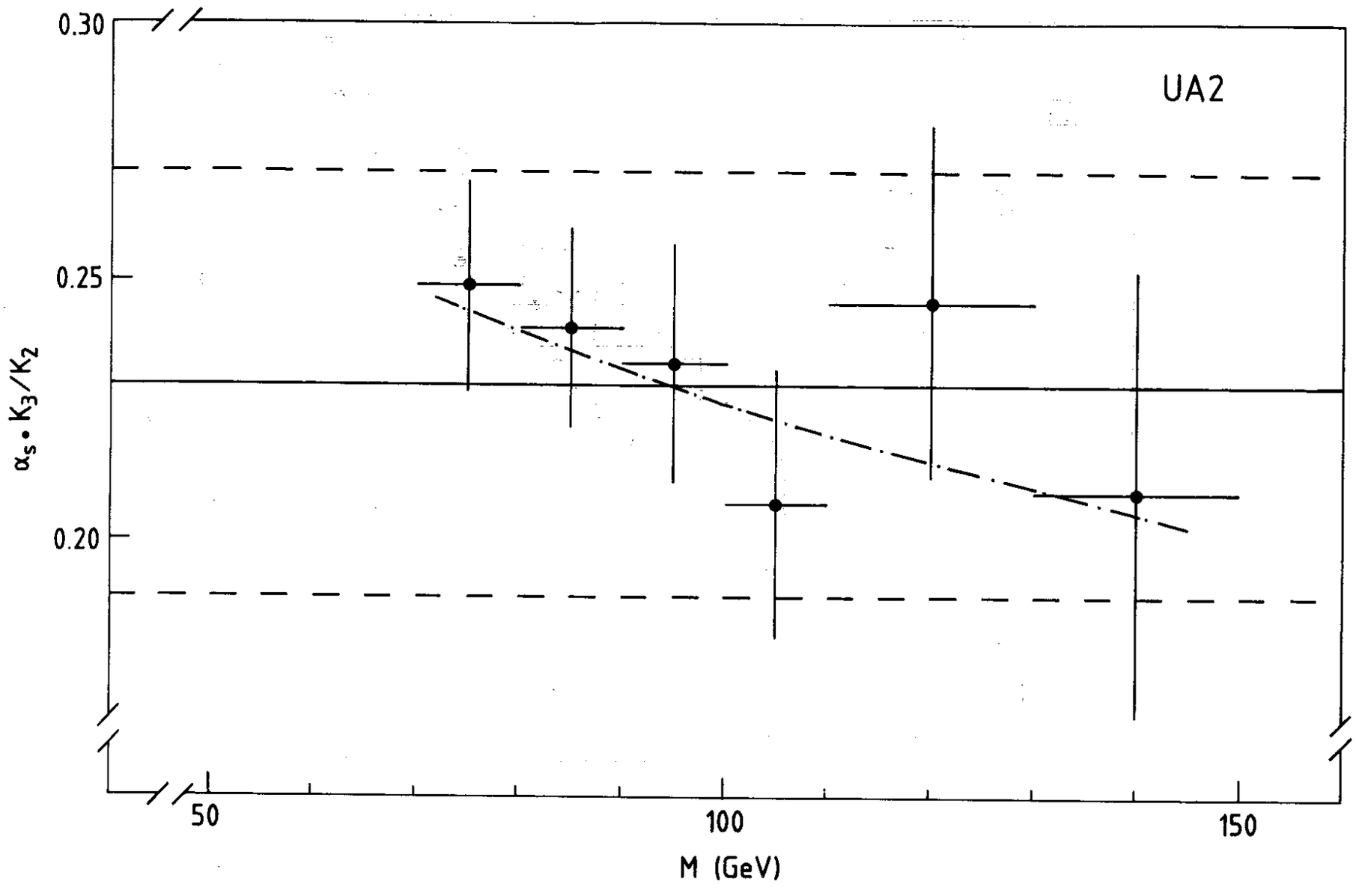

Fig. 8